Available online at www.sciencedirect.com
SCIENCE DIRECT®
Polymer 44 (2003) 5927–5935
polymer
www.elsevier.com/locate/polymer

A study of the large strain deformation and failure behaviour of mixed biopolymer gels via in situ ESEM

R. Rizzieri, F.S. Baker, A.M. Donald*

Polymers and Colloids Group, Department of Physics, Cavendish Laboratory, University of Cambridge, Madingley Road, Cambridge CB3 0HE, UK

Received 20 February 2003; received in revised form 28 April 2003; accepted 28 April 2003

Dedicated to Prof. Ian M. Ward on the occasion of his 75th birthday

Abstract

A mixed biopolymer gel, consisting of a protein (gelatin) and polysaccharide (maltodextrin) mixture has been investigated. By controlling the composition it was possible to construct an 'emulsion-like' structure, with included spherical particles of one phase (maltodextrin) within a continuous matrix of the second (gelatin). Large strain deformation and failure behaviour of this system has been examined via in situ environmental scanning electron microscopy (ESEM). ESEM has been employed to explore the changes in the structure of the material, whilst allowing the sample to stay hydrated as it was subjected to tensile strain, thereby allowing simultaneous imaging and determination of stress–strain data of the native sample. Ductile behaviour was observed, which has been attributed to the stretching, tearing and fracture of gelatin ligaments and debonding at the interface between the maltodextrin particles and continuous gelatin matrix. Deformation and fracture of the maltodextrin particles during tensile testing was also observed. The interfacial fracture energy of the composite has been calculated following an elastomer composite-debonding model, although there are several limitations to this approach for the mixed gel. It was found in samples tested after different ageing times that the debonding stress and strain was decreasing with ageing leading to a lower interfacial fracture energy. Samples were also tested after successive loading cycles, which resulted in a mechanical strength decrease after each cycle.
© 2003 Elsevier Ltd. All rights reserved.

Keywords: Mixed biopolymer; Large strain deformation; Environmental scanning electron microscopy

1. Introduction

The general experimental approach of combining mechanical deformation tests with concurrent dynamic structure visualisation has been used in the past principally to study inorganic materials [1]. In the case of hydrated soft-solid biopolymer systems it is of interest to examine these materials in their natural state, in such a way that structural evolution due to mechanical or thermal perturbation can be followed. Currently, the deformation and failure response of mixed biopolymer gels is not well understood. However, several attempts have been made to characterise and model the deformation and failure mechanisms that may be operating in these materials [2]. Plucknett et al. [3,4] have presented results for large deformation and ductile behaviour of the same mixed biopolymer system studied here. The confocal laser scanning microscopy (CLSM) technique used by Plucknett et al. [3] had the limitation of not controlling the environment around the sample during mechanical deformation. In the present work the temperature and humidity of the sample under test were carefully controlled to avoid dehydration during the experiment. For biopolymer gels solvent loss is a very important issue that can change completely the structure and the behaviour of these materials [2]. In order to understand the failure mechanisms operating in this composite biopolymer system, results from large strain deformation and failure behaviour have been examined simultaneously while structural changes were imaged in an environmental scanning electron microscope (ESEM). Emphasis has been placed upon dynamic observation of deformation and fracture, with mechanical tension tests performed in situ in the ESEM. However, the ESEM permits restricted views of the surface of the sample, while CLSM can penetrate as deep as ~100 μm. A combination of both techniques is therefore suggested.

The ESEM has been employed for this study since it is a powerful analytical tool to explore structural changes in many complicated systems while controlling their

* Corresponding author. Tel.: +44-1223337382; fax: +44-1223337000.
E-mail address: amd3@phy.cam.ac.uk (A.M. Donald).

0032-3861/03/$ - see front matter © 2003 Elsevier Ltd. All rights reserved.
doi:10.1016/S0032-3861(03)00543-3

environment. The ESEM, like all scanning electron microscopes (SEM), offers the possibility of imaging specimens at high resolution and good depth of focus. However, there are important advantages compared to standard SEM [5], which greatly increases the range of specimens that can be examined and the types of investigations that can be performed. The ESEM allows the study of moist material as close to its natural state as possible, in such a way that structural evolution due to mechanical perturbation can be visibly followed [6,7]. In the present study typical working conditions were sample temperature of 2 °C and a pressure of water vapour in the ESEM chamber of 5 Torr (6.7 mbar). By varying either the pressure or the temperature, the relative humidity in the vicinity of the sample can be controlled [5]. Thus, it is possible to obtain images of a material at variable but controlled relative humidity. If the specimen temperature is held constant, decreasing or increasing the pressure of water vapour results in condensation or dehydration, respectively. This ability to control the hydration state of a specimen permits the exploration of a large number of systems. Moreover, without the need for a conductive coating, a range of dynamic experiments can be performed on insulating samples [6,7]. Furthermore, when water vapour is used as the imaging gas, samples can be tested dynamically at different levels of hydration.

This paper describes the results of large strain deformation and fracture of gelatin gels using a tensometer built to fit inside the ESEM chamber and which is capable of dealing with moist samples stretched to large strains. The tensometer has been fitted in the ESEM before [6,7], but in this case the instrument has been modified to keep the sample moist during the entire application of the strain [8]. The temperature and humidity of the specimen as well as force and displacement at given displacement rate were all monitored throughout the duration of the test. ESEM represents a significant advancement in the field of microfracture mechanics of moist materials.

2. Materials and methods

Phase separated gelatin/maltodextrin composite gels, consisting of spherical 'maltodextrin-rich' inclusions within a continuous 'gelatin-rich' matrix phase were investigated during this study. The materials were supplied as dry granular powder by Unilever Research Laboratory, Sharnbrook, UK. Gelatin solutions were prepared by dissolving the powder at 60 °C for 30 min in de-ionised water (containing 0.1 M NaCl). Sodium azide (~500 ppm) was added to prevent bacteriological degradation of the gelatin. Maltodextrin solutions were also prepared by dissolving the powder in de-ionised water at 98 °C and stirring vigorously for 30 min. The mixed gelatin/maltodextrin samples were formed within the incompatibility domain of this system [4]. Phase separated composite samples were made by mixing the two biopolymer solutions, prepared as described above, at 60 °C for 2 min approximately, stirring the mixture slowly with a magnet-stirrer. The composition was 12% w/w of gelatin and 12% w/w of maltodextrin, each phase containing a small fraction of the other biopolymer [4]. The solution was poured onto an aluminium frame fixed on an aluminium mould covered with Parafilm M® to prevent sticking. The mould was kept at room temperature. An aluminium plate covered in Parafilm M® was placed on the solution to seal the sample and a weight of about 500 g located on the top to ensure uniform thickness of the sample. The mould was then stored in the refrigerator at 7 °C for 24 h prior to testing. Some samples were left in the refrigerator for longer, to monitor the effect of ageing on the maltodextrin/gelatin composite. Samples were tested after 1 day, 1 week, 1 month and 2 months, respectively.

Samples were cut from the thin gelled sheet using a 'dog-bone' shaped cutter (10 mm gauge length and 4 mm width). The sample was then glued using a cynoacrylate adhesive on one side of two aluminium specimen holders. As can be seen from Fig. 1, the sample was glued onto flat aluminium strips punctured such that they could be dropped over pegs mounted on both jaws of the tensometer, one of which was attached to the load cell. The sample was laid down so that it was in contact with the cooled bar, but only until the strain was applied. As the extension proceeded the sample lifted up slightly from the cooling block. It is assumed that this occurred because sticktion between the clamps and the pegs did not accommodate the thinning of the sample as it stretched. As stretching advanced the sample distance from the cooling block (approximately 1 mm) was constant during the test. This small distance between the sample and the cooling stage prevented any interference to the measurements due to stick-slip and water condensation on the sample, yet ensured good temperature control of the sample. Prior to running the experiment the cooling block, responsible for keeping the sample at a controlled temperature during the whole experiment, was equilibrated at the test temperature of 2 °C. Tensile tests were performed at a strain rate of approximately 0.001 s^{-1} at controlled humidity and temperature.

Specimens were imaged using an ElecroScan 2010 ESEM equipped with a tungsten hairpin filament. The beam energy was 20 kV and signals were collected using a gaseous secondary electron detector (GSED). Geometric constraints of the mechanical stage limited the working distance to no less than 8.5 mm. Water vapour was used as the imaging gas, with constant pressure of approximately 5 Torr. The temperature was maintained at 2 °C during pump-down and the duration of the whole experiment. The experimental conditions and an accurate description of the tensometer built for these experiments are fully described in Rizzieri et al. [8]. This construction permitted load-extension curves to be determined for hydrated samples simultaneously with imaging and maintaining the sample in its fully hydrated state, providing a unique opportunity to

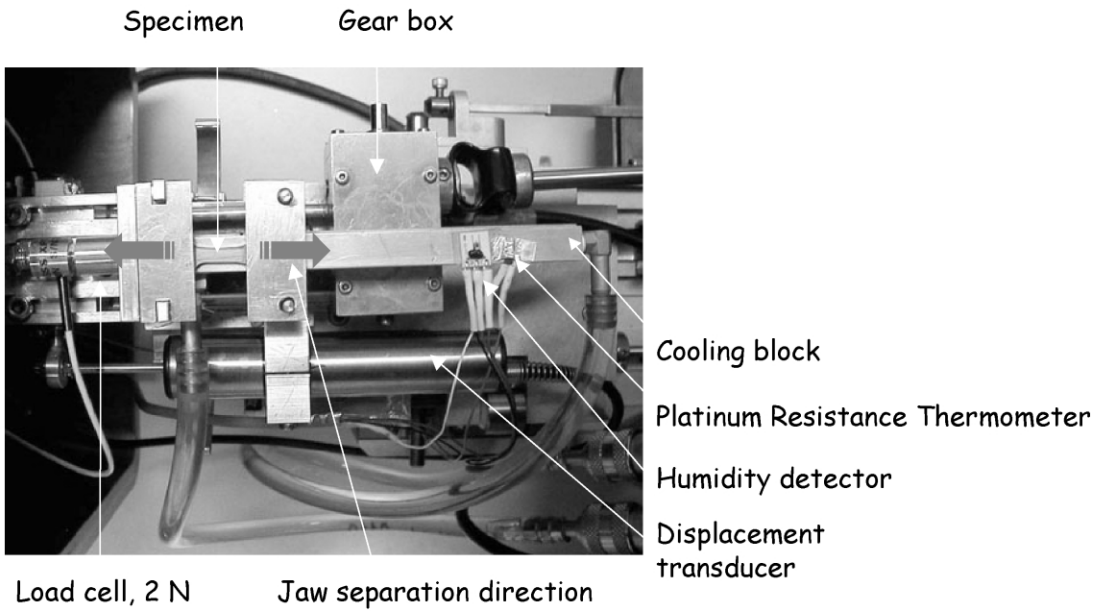

Fig. 1. Photograph of the tensometer used, with its components for testing samples within the specimen chamber of the ESEM. The black arrows indicate the direction of the jaw separation. The gearbox is connected to a stepper motor attached to the door of the ESEM chamber. The 'dog-bone' shaped gelatin sample is glued onto the aluminium specimen holders, designed to be dropped onto the tensometer. The shape of a 'dog-bone' is obtained by pressing on the gelatin a specially designed steel 'cookie' cutter. The sample is in contact with the cooling block before starting the test. Once the strain is applied the sample lifts itself up by about 1 mm from the cooling block. Only the initial part of the stress–strain curve (approximately for the first 0.1% strain) is corrupted by the sample stick-slipping on the cooling block. A more detailed explanation can be found in Ref. [8].

explore the structure and dynamic mechanical characteristics of moist systems, such as gelatin-containing gels. During all the tests the experimental conditions were kept identical to compare the results.

For materials that exhibit relatively large strain failure (i.e. $>10\%$), such as gelatin gels, correction must be made for the reduction in cross-sectional area that occurs during deformation [9]. The corrected failure stress, named 'true' stress, is defined as the load (F) divided by instantaneous cross-sectional area (A) :

$$\sigma_T = F/A \tag{1}$$

For the gelatin gels studied in the present work the deformation during tensile testing can be approximated to occur at constant volume, and so A can be related to the original cross-sectional area A_0 through the equation:

$$AL = A_0L_0 \tag{2}$$

where L and L_0 are the original and instantaneous gauge lengths, respectively. The true stress is thus defined as:

$$\sigma_T = FL/A_0L_0 \tag{3}$$

Similarly, the corrected failure strain, termed 'true' strain is approximated by:

$$\varepsilon_T = \ln(L/L_0) \tag{4}$$

The elastic modulus in tension can then be calculated by:

$$E_T = \sigma_T/\varepsilon_T \tag{5}$$

During this study the parameters that identified the level of damage occurring during deformation are 'true' stress and 'true' strain, however, the instantaneous gauge lengths (L) was assumed to be the same as the distance between the clamps.

3. Results and discussion

An ESEM image of the unstrained mixed biopolymer sample is shown in Fig. 2. The continuous phase is gelatin while the spherical inclusions are maltodextrin particles. A homogenous distribution of the particles inside the matrix

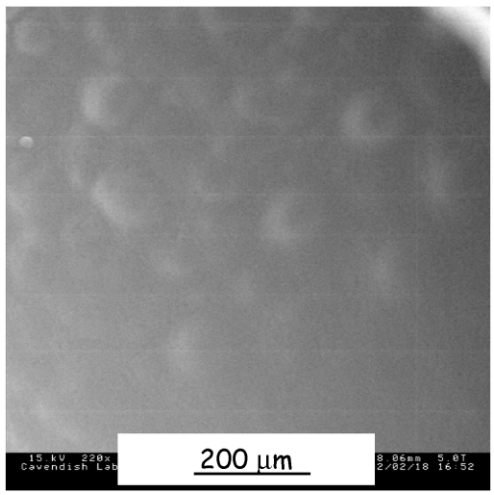

Fig. 2. ESEM image of an unstrained mixed biopolymer sample, the continuous phase is gelatin while the spherical inclusions are maltodextrin particles.

was observed, with the particle size varying from approximately 50 to 150 μm in diameter. An approximate average particle diameter of 100 μm was adopted here for the calculations below. The maltodextrin inclusions inside the gelatin matrix were not very clear in most of the ESEM images taken during this study of the unstrained sample. The preparation and storage of the phase-separated composite system are thought to be the reason for a thin film of the matrix continuous gelatin to form at the top of the sample. This could be due to falling under gravity of the dispersed phases inside the sample and presumed lower surface tension of the liquid gelatin matrix during cooling. Consequently many micrographs taken of the top storage-surface of the sample show the continuous gelatin matrix with little topological evidence of spherical maltodextrin particles located under the gelatin skin. A comparison between top and bottom storage-surface is presented in Fig. 3, showing the much greater visibility of particles on the lower surface. The contrast between the particles and the bulk phase in all the images presented here appear to result mainly from surface topography [17], although it is not inconceivable that differences in the polymers themselves could cause contrast [5].

A series of ESEM images showing the typical evolution of the surface morphology of a mixed biopolymer gelatin/maltodextrin system recorded simultaneously whilst applying strain is shown in Fig. 4. These images clearly illustrate the phase-separated nature of this material during applied strain. Arrows in Fig. 4(A) shows the direction of the applied strain for both the tensometer and the micrograph, and these directions are constant for all micrographs. A characteristic corrected tension true stress/strain curve is also shown in Fig. 4. Three different load regimes were observed to be representative of the mixed biopolymer behaviour under applied strain at constant jaw separation rate. At low strains ($<20\%$) no change in the surface morphology was observed. The micrograph looked identical to the ones taken of the unstrained sample. At approximately 40% strain, debonding of the maltodextrin particles from the matrix became apparent at the surface of the sample, as shown in Fig. 4(B). The maltodextrin debonding seemed to occur, in accordance with Plucknett et al. [3], at the shoulder of the true stress/strain curve. Clear

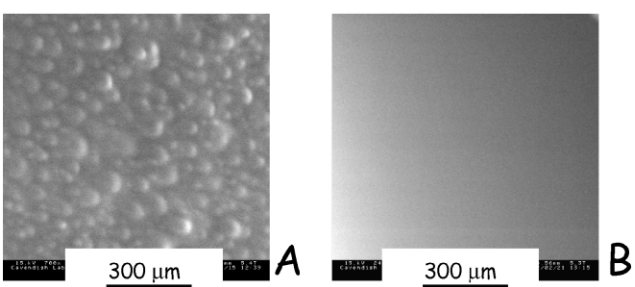

Fig. 3. Comparison between the bottom (A) and top (B) surface of a phase-separated gelatin/maltodextrin composite sample after being stored for 24 h in the refrigerator at 7 °C inside the aluminium mould.

visual evidence of debonding, like the one in Fig. 4(B) has not always been observed during this study. Some samples presented no surface evidence of debonding until a crack opened on the surface revealing the deformation and fracture mechanism behaviour occurring in the composite. In Fig. 4(C) a crack formed on the gelatin surface thereby showing what was happening inside the sample and demonstrating the dynamics of the failure mechanisms operating in the mixed biopolymer sample.

When the surface was governed by the presence of a predominant layer of gelatin skin, at large strain deformation ($>20\%$) a series of regular bands aligned along the direction of the applied strain appeared, as shown in Fig. 5. It is the first time that this unexpected morphology has been reported. At the present the most likely interpretation of this phenomenon is thought to be buckling of the gelatin surface skin, stiffer than the interior, due to slight loss of water. Buckling is a kind of mechanical instability due to a combination of various external causes: in this case the applied strain on a moist gelatin sample constrained at the edge by the clamps, is sufficient to explain the buckling phenomenon. A more detailed explanation supported by quantitative results and measurements taken from different techniques and a mathematical model of what it thought to be the reason for the formation of the bands is to be presented in Rizzieri et al. [10].

A series of ESEM images of the structural evolution of a gelatin/maltodextrin composite with increasing applied strain is shown in Fig. 6. The direction of the applied strain is vertical. The presence of two air bubbles helped to focus the attention on the same position as the test proceeded. A crack was initiated on the surface from some defect (e.g. a small particle, an impurity, crack tips developing inside and running to the surface, etc.). The air bubbles became thin and elongated due to the applied strain and lateral contractions, until a crack propagated from one air bubble to the other. Once the crack reached the second air bubble the crack partially stabilised in lateral expansion and started opening in the direction of the applied strain. The expansion of the crack revealed the main mechanism thought to be responsible for the ductile behaviour of this material. It can be seen that the gelatin formed string-like bridges between the edges of the crack. Tearing, stretching and failure of the gelatin ligaments is believed to account for most of the strain hardening behaviour shown in the stress–strain curve in Fig. 4. The presence of a second phase acting as regularly distributed rigid defects in the continuous soft matrix impeded the propagation of cracks and hence made crack propagation more difficult. However, it is known [9] that rigid fillers in reinforced polymers can give rise to flaws, which can reduce both the fracture strength of the polymer and the elongation to failure. The strength of the matrix/particle interfacial is crucial in dictating the stress regime inside the composite. In the present case the interface is believed to be weak enough for the stress to concentrate at the equators of the particles during mechanical deformation,

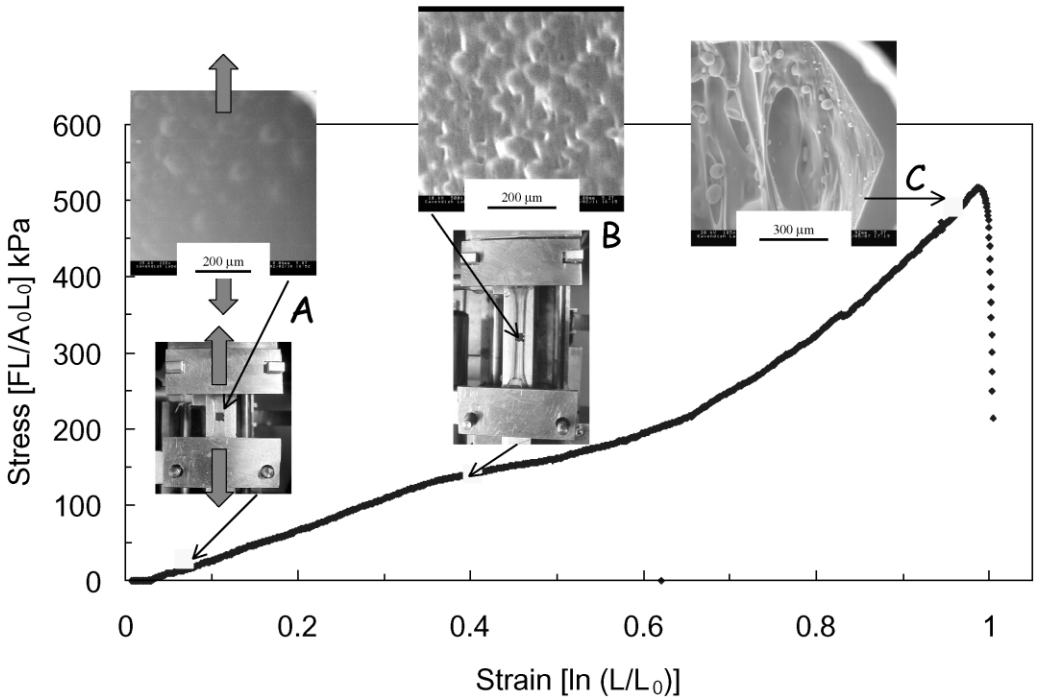

Fig. 4. In situ stress–strain plot for a 'typical' tensile test on mixed gelatin-maltodextrin sample in the ESEM. Three characteristic points during the tensile tests are illustrated on the top of the diagram, each with an ESEM micrograph of the mixture surface during stretching. The direction of the applied strain is vertical. (A) At low strain the sample surface is identical to the one of an unstrained sample. (B) At about 50% strain the sample surface shows the presence of debonded maltodextrin particles. (C) At breakage the surface sample is mainly dominated by the fibrillated gelatin matrix.

which is similar to the stress concentration found around holes and notches in plates [11]. The presence of the stress concentration can lead the gelatin matrix to deform throughout a large volume of material. Hence the composite absorbs a large amount of energy during deformation but before fracture. The exact mechanisms of deformation around the particles depend upon the conditions of testing, i.e. temperature and deformation rate. The deformed mixed gelatin structure is shown in Fig. 6, where many gelatin strands are seen to stretch, helping each other to support the stress until the final failure of the whole sample.

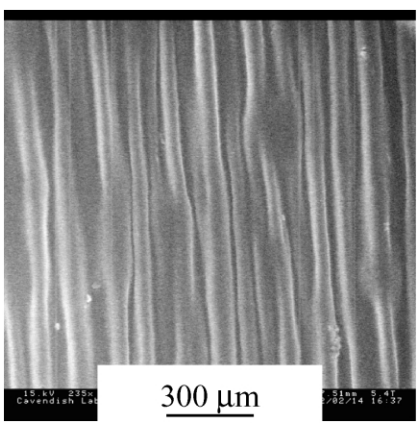

Fig. 5. ESEM micrographs showing the presence of regular bands on the surface of the mixed biopolymer system which has a layer of gelatin on the top surface. The direction of the applied strain is the same as the direction of the bands. A detailed explanation of this phenomenon can be found in Ref. [10].

In Fig. 7 debonding, deformation and breakage of maltodextrin particles can be seen. Debonding localised at the pole of the particle is clearly shown as the voids elongate. Where the maltodextrin particles became visible, (i.e. when the surface skin is very thin or absent) they were found sometime to be deformed into an oval shape, the long axis pointing in the direction of the applied strain. This was not observed for CLSM experiments conducted by Plucknett et al. [3] and during ESEM tests, where a crack was initiated by notching the sample. In the case of large strain deformation observed in situ in a CLSM [3] it was not possible to focus on fractured particles due to limitations in resolution. During ESEM measurements of a notched sample the particles were seen to debond ahead of the crack; but they preserved their spherical shape, as shown in Fig. 8. The main reason for the discrepancy is attributed to the different loading condition. When a sharp crack is created the stresses concentrate at the head of it, and a small strain (in many cases still in the elastic region) is enough to open and propagate the crack through the sample [11]. During this study unnotched specimens were stretched and cracks were observed to occur at large strain deformation ($>40\%$). In this case it is believed that the cracks developed only after large uniform distribution of stresses along the sample gauge length [12]. Consequently, the interfacial strength and the difference in stiffness between the particle and matrix dictate the deformation process. In Fig. 7 a crack

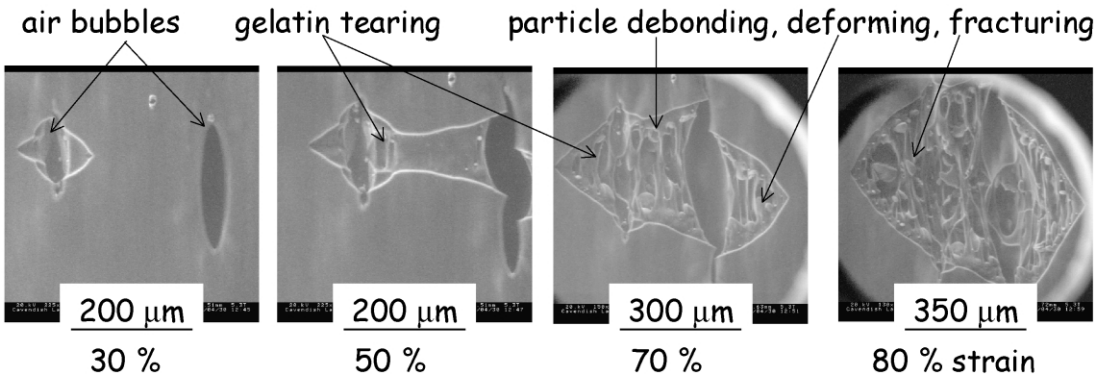

Fig. 6. ESEM micrographs following the opening of a crack on the surface of a mixed gelatin sample. The crack propagated from an existing defect on the surface. As the crack opened, it revealed the underlying maltodextrin particles. The gelatin matrix fibrillated around the particles until complete failure of the sample. The morphology of the specimen is shown in its complexity only after breakage of the surface. The fact that the micrographs were taken at a frame refresh rate of 0.5 frames s^{-1} and the strain rate applied was low (10 µm s^{-1}), allowed us to follow and store good images of the surface as the sample failed.

across the particle is observed to run perpendicular to the stretching direction. Particles were sometimes observed to undergo deformation and eventual debonding with increasing applied strain (at strain >40%). The interfacial fracture energy calculated using the debonding/void mechanisms for elastomeric composites [13] is considered as an estimate of the interfacial fracture energy, G, according to the following [9]:

$$G \sim \sigma^2 r/E_C \tag{6}$$

where the debonding stress, σ, is known for a particle of radius, r, within a composite mixed biopolymer matrix of elastic modulus, E_C.

The composite mixed biopolymer elastic modulus was derived from Eq. (5) on true stress/strain data from Fig. 9. The debonding stress (σ) was estimated in the vicinity of the maximum curvature of the shoulder shown in the true stress/strain plots. This procedure is only an approximation deriving both from ESEM indication of debonding at a given strain, and CLSM results from Plucknett et al. [3]. The average particle diameter ($2r$) was estimated to be ~100 µm, from averaging results from several ESEM images. The values of G, σ and E_C are presented in Table 1. Fig. 9 shows the difference in mechanical behaviour between samples aged for different times. The four curves reported in Fig. 9 are representative of the average behaviour obtained from samples cut out from the same moulded mixed gelatin sheet, after 1 day, 1 week, 1 month and 2 months ageing time. The experiments were repeated twice for each sample condition and a good reproducibility was observed: the two curves coincided at strain below fracture and the curve which gave the lower fracture strain was then reported in Fig. 9. However, results from samples aged at the same time and tested under the same condition, but cut from different moulded mixed gelatin sheet, were not superposable. It is believed that many parameters, such as temperature and humidity during preparation, storing and handling influence the mechanical behaviour of the resulting material.

By increasing the ageing times the sample debonding stresses decrease, as shown in Fig. 9 and Table 1. Equally, composite elastic modulus increases with increasing storage

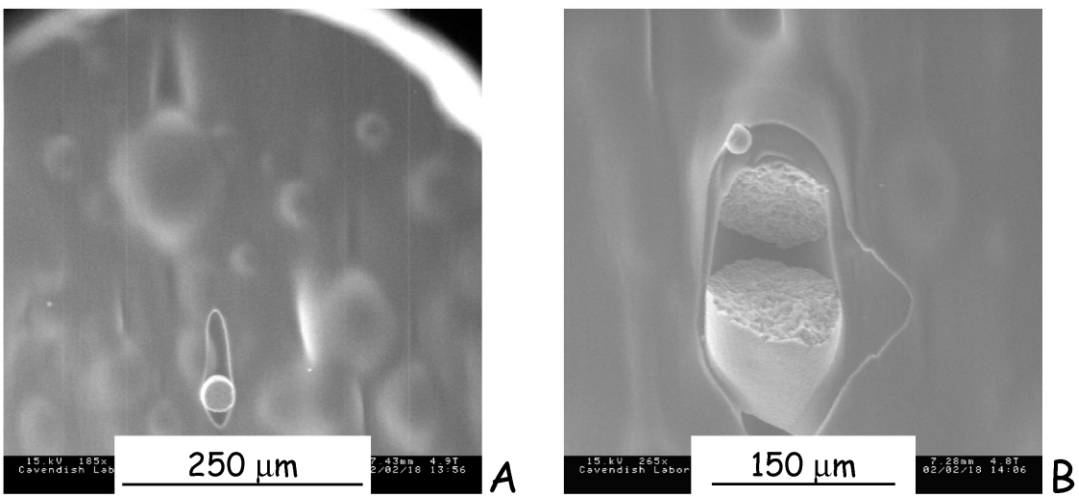

Fig. 7. ESEM micrographs following a maltodextrin particle debonding and cracking due to the applied tensile strain.

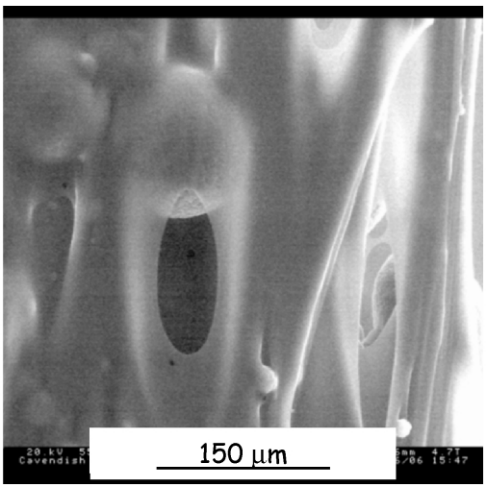

Fig. 8. A debonded maltodextrin particle during a tensile test in situ in ESEM of a notched mixed biopolymer sample. The particle is spherical and it does not exhibit deformation or fracture.

time, as presented in Table 1. From data shown in Fig. 9 it is possible to compare the interfacial fracture energy, obtained from Eq. (6), of the composite systems at increasing ageing times. The results obtained are presented in Table 1; they show that increasing storage time corresponded to a decrease in interfacial fracture energy. These results can explain the lower interfacial fracture energy found by Plucknett et al. [3] after testing the same system in an uncontrolled environment. The interfacial fracture energy found by Plucknett et al. [3] is equivalent to the one found here for samples aged over 2 months. Further examination under ESEM of the failure surfaces of samples aged for 1 day and 1 week revealed evidence of fractured maltodextrin particles. No fractured particles were found on the failed surface of samples aged for 1 or 2 months, confirming the decrease in interfacial fracture energy with storage time.

However, the approximate nature of Gent analysis [13] ignores interparticle interactions (interaction of the stress field around each particle) and particle deformation (the phase-separated particles are not rigid), which are both important effects occurring in mixed biopolymer gels. This

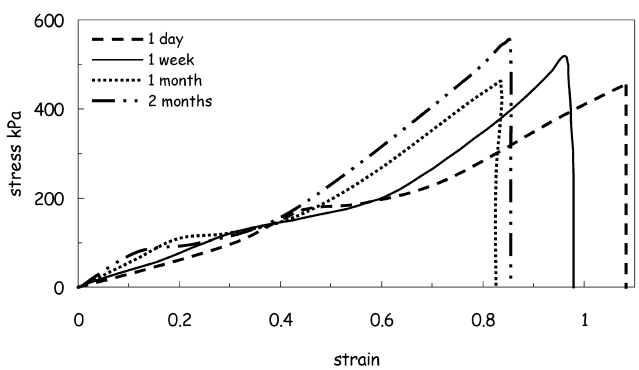

Fig. 9. Comparison of true stress/true strain plots of samples left to age for different times. The samples were stored in a fridge at 7 °C for 1 day, 1 week, 1 month and 2 months before testing.

Table 1
Debonding stress (from plots in Fig. 4) and interfacial fracture energy (from Eq. (6)) for samples stored in a fridge at 7 °C 1 day, 1 week, 1 month and 2 months, respectively before testing.

	1 Day	1 Week	1 Month	2 Months
σ (kPa)	180	160	120	80
E_C (kPa)	200	300	600	700
$G \sim \sigma^2 r/E_C$ (J/m^2)	8.1	4.3	1.2	0.4

study presents evidence of particle deformation and fracture which indicates that any quantitative estimate of interfacial fracture energy, based on Eq. (6) must be treated with considerable caution, although probably permitting correct trends to be deduced.

It is believed that the increase in the composite elastic modulus with time is due to an increase in gelatin stiffness. Based upon deformation studies of bulk gelatin gels, Bot et al. [2] indicated that network cross-link formation occurs during ageing, and this is substantiated by rheological measurements [14]. This phenomenon is thought to be responsible for the increased stiffness of the gelatin matrix with time, which controls the elastic modulus of the composite. However, the decrease in interfacial fracture energy with ageing times is not completely understood. The increase in network cross-linking is believed to have a great effect on the interdiffusion of polymer chains at the interface during ageing. It is known that when two non-gelling polymer surfaces are in contact, the polymer chains are free to diffuse across the interface [15]. If the molecular weights are sufficiently high, physical entanglements of the inter-diffusing polymer chains may arise. As a consequence, the interfacial strength will be dependent upon factors such as the respective polymer molecular weights, the area density of the polymer chains and the contact (or ageing) time of the interface. For the case of gelled layers in contact, the network nature of the polymer needs to be taken into account. Only limited polymer diffusion is possible for what may be considered ‘permanent’ bridges across the interface [2]. However, an additional factor may need to be considered for these samples. At early times the phase separation between matrix and particle may not have reached equilibrium. This will also favour chains bridging the interface and enhancing the interfacial strength. As time proceeds, the interface will tend to sharpen due to the unfavourable entropy of mixing, and as this occurs a drop in interfacial strength may also be expected.

For the present example, it is shown that the interfacial fracture energy for gelatin/maltodextrin depends on ageing. For newly made samples (1 day to a week old) the interfacial fracture energy was higher than for matured samples (1 or 2 months), which implies structural development for this system during ageing. This is attributed to a reduction in the number of chains bridging the interface as network formation and a further push towards equilibrium phase compositions (which may include a redistribution of

water) both favour a sharpening of the interface. Systems in which gelation and phase separation occur simultaneously are known to have complex time dependences and interactions [16], but in this instance both effects will have the same effect of weakening the interface between the particle and matrix. This is also consistent with the Gent analysis [13], which states when as the composite modulus increases the interfacial fracture energy should decrease ($G \sim 1/E$) but which ignores other additional effects which may be important here.

Fig. 10 shows a series of straining cycles of a mixed gelatin/maltodextrin sample. It was observed that most of the deformation strain was recovered upon unloading the sample before subsequent cycles. However, a small permanent strain of ~10% was retained in the composite sample after each cycle. Furthermore, Fig. 10 presents a lowering of the debonding stress for successive cycles ($\sigma \sim 300$ kPa after 1 cycle, $\sigma \sim 220$ kPa after 2 cycles and $\sigma \sim 200$ kPa after 3 cycles) whereas, the composite elastic modulus was increasing. The interfacial fracture energy (calculated from Eq. (6)) decreased after each cycle (from ~4.5 J m^{-2} after 1 cycle, to ~1.2 J m^{-2} after 2 cycles and to ~0.5 J m^{-2} after 3 cycles). The mechanical behaviour observed during successive cycles on the mixed biopolymer sample was similar to the one observed after increasing ageing time. The decrease in interfacial energy after each cycle is attributed to the debonded maltodextrin particle interfaces, which may not fully re-heal after subsequent cycles (in accordance with Plucknett et al. [3]).

4. Conclusions

A new method has been developed whereby quantitative stress–strain data has been obtained for mixed gelatin/maltodextrin gels in their natural (hydrated) state, together with simultaneous imaging of structural evolution and failure mechanisms during large strain deformation. Dynamic observations of the microstructure response to mechanical deformation in systems kept hydrated throughout the whole experiment have been carried out in situ in the ESEM. By using an ESEM fitted with a tensometer capable of keeping a sample moist over large strains and long times, it was possible to observe hitherto unreported structural changes in the mixed gelatin-based system subjected to uniaxial tension. It was shown that the gelatin matrix was tearing during stretching, bridging across cracks as they formed, and particles of maltodextrin included in the gelatin underwent deformation and fracture. Comparison of the mechanical response of samples aged for increasing time before testing and samples subjected to various loading cycles were also made.

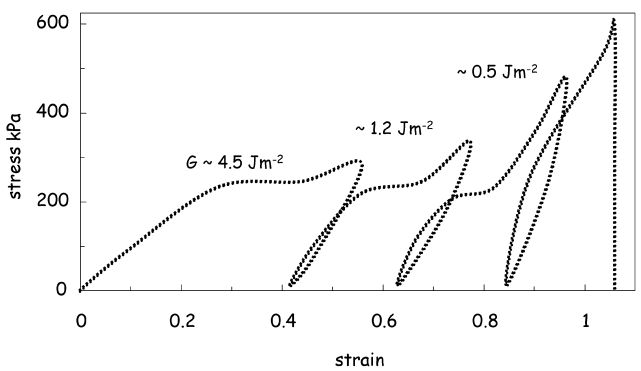

Fig. 10. Plot of 4 strain cycles of a mixed biopolymer sample tested in situ in the ESEM.

Such observations have led to an appreciation of the limitations of previous models due to insufficient knowledge of microstructural changes occurring during deformation. Samples tested at increasing ageing times were found to decrease in interfacial strength with debonding occurring at lower stresses. This behaviour is believed to arise from the extent of polymer interdiffusion across the interface and network formation occurring concurrently in the system during ageing. Moreover, the uncrosslinked structure of the maltodextrin and the minimal mutual 'solubility' of each phase inside the other are both effects that contribute to the loss in interface strength as sharpening of the interface proceeds. After cycling the composite material was also found to increase in elastic modulus and decrease in interfacial fracture energy; the weakening of the interface here was attributed to incomplete healing of the interface even though substantial strain recovery occurs after each cycle. An elastomer composite debonding model was adopted to calculate the debonding stresses and interfacial fracture energy. The limitation of the model requires novel investigations and approaches to investigate better these phenomena.

Acknowledgements

The authors thank the Product Microstructure Division of Unilever Research Colworth for their support of this research programme, and for permission to publish this paper. This paper is dedicated to Professor Ward, whose work over many years aimed at understanding polymer deformation has proved so vital, not only to our knowledge, but also to the health of the community working in this area.

References

[1] Moller CV, Healy JC, Mai YW. Fatigue Fract Engng Mater Struct 1994;17:285–96.
[2] Bot A, van Amerongen IA, Groot RD, Hoekstra NL, Agterof WGM. Polym Gels Networks 1996;4:189–227.
[3] Plucknett KP, Normand V, Pomfret SJ, Ferdinando D. Polymer 2000; 41:2319–23.
[4] Plucknett KP, Normand V. Polymer 2000;41:6833–41.
[5] Baker FS, Craven JP, Donald AM. Techniques for structural characterisation of polymers. London: Wiley; 2003. Chapter 4.

[6] Thiel BL, Donald AM. J Texture Stud 2000;31:437–55.
[7] Stokes DJ, Donald AM. J Mater Sci 2000;35:599–607.
[8] Rizzieri R, Baker FS, Donald AM. Rev Sci Inst. in press.
[9] Young RJ, Lovell PA. Introduction to polymers, 2nd ed. London: Chapman & Hall; 1991. Chapter 5.
[10] Rizzieri R, Mahadevan L, Donald AM. Manuscript in preparation.
[11] Williams JG. Fracture mechanics of polymers. Chichester: Ellis Horwood; 1994. Chapter 5.
[12] Kinloch AJ, Young RJ. Fracture behaviour of polymers. Applied Science: London; 1983. Chapters 3 and 11.
[13] Gent AN. J Mater Sci 1980;15:2884–8.
[14] Djabourov M. Contemp Phys; 29: 273–297.
[15] Brown HR. Annu Rev Mater Sci 1988;21:463–89.
[16] Tromp HR, Jones RAL, Rennie A. Macromolecules 1995;28: 4129–38.
[17] Toth M, Thiel BL, Donald AM. Ultramicroscopy 2003;94:71–87.